AD-A137 401 ANALYSIS AND COMPUTATIONS OF MICROWAVE-ATMOSPHERIC INTERACTIONS(U) CALIFORNIA UNIV DAVIS PLASMA RESEARCH GROUP W WOO ET AL. 31 AUG 82 PRG-R-92 N00019-81-C-0507 1/1

UNCLASSIFIED F/G 20/9 NL

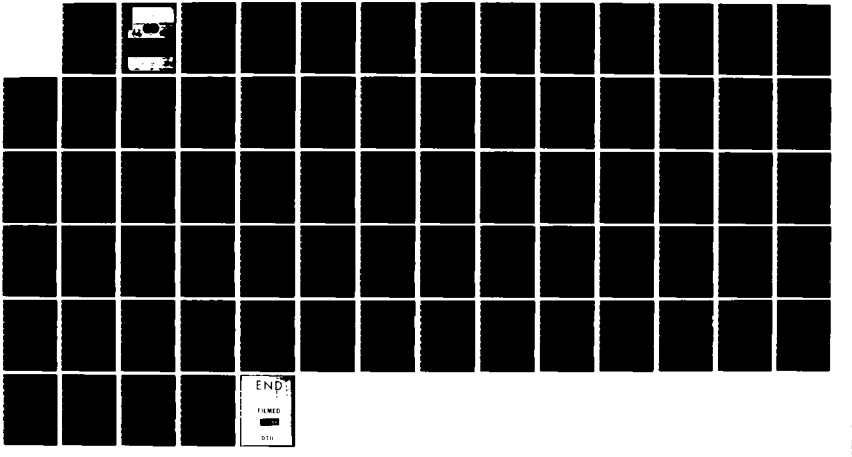

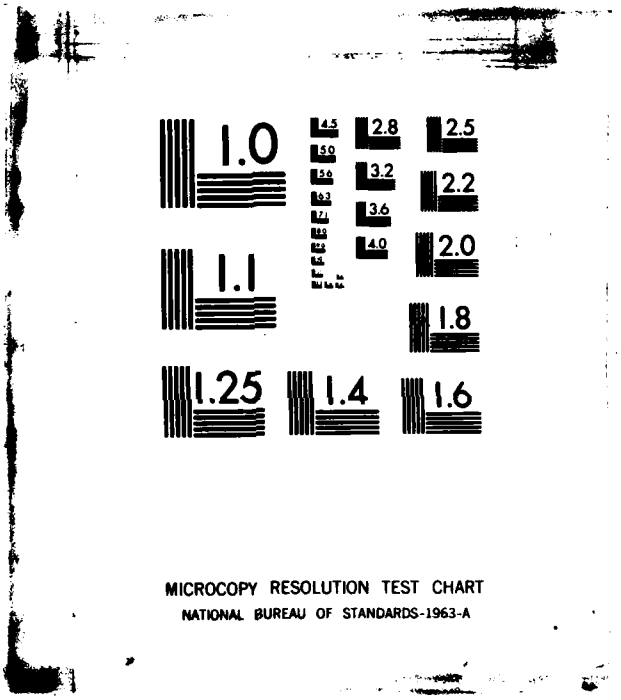
1.0
1.1
1.25
1.4
1.6
1.8
2.0
2.2
2.5
2.8
3.2
3.6
4.0
4.5
5.0
5.6
6.3
MICROCOPY RESOLUTION TEST CHART
NATIONAL BUREAU OF STANDARDS-1963-A

University of California, Davis

UCD

ANALYSIS AND COMPUTATIONS OF MICROWAVE-ATMOSPHERIC INTERACTIONS

Wee Woo, Senior Investigator
and J. S. DeGroot, Principal Investigator

Final Report for the Period September 1, 1981 to August 31, 1982

NAVAIR 00019-81-C-0507

PRG R-92

Department of Applied Science
Plasma Research Group

TABLE OF CONTENTS

I. INTRODUCTION

The Plasma Research Group of the University of California at Davis continued the theoretical work of microwave-atmospheric interactions, in close coordination with personnel at the Naval Research Laboratory and elsewhere. This report covers the period September 1, 1981 to August 31, 1982. We have made advances in two areas: (1) expanding the previous survey into new regimes; and (2) simulations of recent NRL focused microwave experiments. The main results of our invesitgation are described in the following. Typical hydrodynamic calculations show that an ionization front is rapidly formed which moves toward the microwave source and consequently decouples the microwaves from the original ionization region. By focusing the microwaves or using a reflector, ionization can be confined to localized regions where the microwave strength is high enough to cause breakdown even though the incoming microwaves are below threshold. In a strongly collisional atmosphere, it is found that the cutoff plasma density, which roughly equals the collisionless cutoff density multiplied by the collisionality, is much higher than the calculated maximum density. This results in high absorption that increases with microwave power, decreases with atmospheric pressure, and is quite independent of other parameters. In a weakly collisional atmosphere, breakdown easily creates a

plasma density higher than the cutoff density and causes reflection. It is found that the reflection decreases with the collisionality of the system and is quite independent of the microwave strength. In general, the microwave field strength in the ionization regions is attenuated to the breakdown value at steady state, and the resulting electron temperature is about 2 eV, independent of the incident microwave flux. Limitations of the calculations are due to the availability of experimental data for the rate coefficients, but comparison to results from recent focused microwave experiments shows excellent agreement.

In the past, most studies and measurements were done[1] near the breakdown thresholds. Recently experiments have been performed , for microwave power higher than the threshold, to study the behavior of the plasma after breakdown. Our investigation will cover the overall scope of the phenomena and will be described in more detail in the following.

If we neglect free electron diffusion, experimental data[1] show that the breakdown threshold is roughly given by $E_{rms} \sim 32 \sqrt{p^2_{Torr} + 2 f^2_{GHz}}$, here E_{rms} is the rms electric field in volt/cm, p is the atmospheric pressure and f is the microwave frequency (the subscripts indicate the units). At sea

level ($p_{Torr} >> f_{GHz}$), the microwave power flux breakdown threshold is about 1.5 MW/cm^2. This kind of power is achievable using present technology. Free electron diffusion is only important in weakly collisional air and at the time of breakdown, and can be ignored once the plasma builds up; this is the stage we are most interested in.

After breakdown, the plasma density grows exponentially in time quickly until the density is high enough for reflection and absorption of the microwaves. The microwave-plasma interaction is basically dominated by electron-neutral collisions (to be described in Section IV), in which the collision frequency is roughly given by $\nu_c \sim 5 \times 10^9 \, p_{Torr}$ at sufficiently high microwave power. In the important frequency range of a few GHz to several hundred GHz the system is very collisional in the lower atmosphere ($\nu_c/\omega >> 1$, where $\omega = 2\pi f$ is the angular frequency of the microwaves). In this case the cut-off plasma density of the microwaves is given by $n/n_c \sim \nu_c/\omega$, here $n = 1.26 \times 10^{-8} \, f^2 \, cm^{-3}$ is the critical density, instead of the usual $n \sim n_c$ in the collisionless case.

We show in this paper that reflection depends mainly upon the height and the slope of the density profile. In the strongly collisional limit, reflection becomes important when

$k_o \ell < 1$ and $n/n_c > \nu_c/\omega$, here k_o is the wavenumber of the microwaves and ℓ is the scale length of the density gradient. In the weak collisional limit, they are given by $k_o \ell < \nu/\omega_c$ and $n/n_c > 1$. In useful atmospheric units, the conditions for the two limits are given by $\ell(\text{cm}) < f_{\text{GHz}}^{-1}$ and $n(\text{cm}^{-3}) > 10^{13} P_{\text{atm}} f_{\text{GHz}}$ valid for $P_{\text{atm}} > 10^{-3} f_{\text{GHz}}$, and $\ell(\text{cm}) < 10^{-2} P_{\text{atm}}^{-1}$ and $n(\text{cm}^{-3}) > 10^{10} f_{\text{GHz}}^2$ valid for $P_{\text{atm}} < 10^{-3} f_{\text{GHz}}$ respectively.

In very collisional air, the condition for good absorption is given by $(n/n_c)(k\,\Delta) > \nu_c/\omega$, here Δ is the width of the density profile. Rewritten into atmospheric units, this is $n\Delta(\text{cm}^{-2}) > 10^{13} P_{\text{atm}}$ or $(n/N)\Delta\ (\text{cm}) > 10^{-6}$, here N is the atmospheric density. Therefore only low ionization of the air is needed to give good absorption.

The currently available experimental data were mainly obtained in dc experiments and are roughly valid in the range $0 < E_{\text{rms}}/P_{\text{Torr}} < 100$ within an accuracy of 10 to 20%. Checking the relation of the data to the kinetic description carefully, we can relate[1] the data to an effective microwave field strength which is defined by $E(1 + \omega^2/\nu_c^2)^{-1/2}$. Therefore the rate coefficients (which are elastic collision, ionization, and attachment) and thermal energy of the electrons, can be determined macroscopically as functions of mi-

crowave field strength without knowing the details of the microscopic kinetic description.

We present hydrodynamic calculations for both planar and spherical geometries. A problem that must be avoided is the growth of the plasma density in all space. After some time the density even grows faster at places close to the microwave source because the field strength is stronger there due to reflection. Eventually the microwaves will be cut-off by a very high plasma density near the source.

In the planar case, we present two types of calculations. First, a local region is pre-ionized by other means, then the pre-ionized plasma grows to high enough density to cause high absorption before the density at other places grows significantly. During this time, a steady state ionization front is formed and moves rapidly toward the microwave source.

Second, a reflector is placed at a boundary, such that standing microwaves are formed in the system. The incoming power is below the breakdown threshold, therefore the problem of cutting-off the microwaves near the source can be avoided. However the maxima of the standing wave can be above the threshold, and the multi-peak plasma density is formed and the microwaves are absorbed. Stationary state absorption is ob-

tained in this case.

In very collisional air, results for both cases show that the product n (sum for multi-peak density) of the asymptotic plasma density profile remains roughly the same at fixed microwave power and atmospheric pressure, and is quite independent of other parameters. Therefore it gives fixed absorption (see Eq. 49). The reason is that the microwaves have to be attenuated to the breakdown value $E_{rms} \sim 32\ p_{Torr}$ in the density profile in order that a steady state is achieved. Thus the required attenuation fixes the product of n and therefore the absorption. Energy that is not absorbed will be transmitted in the pre-ionization case because the density required for significant reflection is not built up.

We also find that the asymptotic absorption increases rapidly with the microwave power and inversely with pressure. Total absorption occurs for power not very much higher than the threshold.

In weakly collisional air, the reflection density is easier to be built up. We also find that the reflection decreases with ν_c/ω, the collisionality of the system, and is quite independent of the microwave strength. The energy that is not reflected will be absorbed due to the longer elongated

density profile at the back in the pre-ionization case.

In spherical geometry, which simulates converging microwaves, the cut-off problem is also avoided because the microwave beams are above breakdown threshold only near the focal region. We find that one after another density peaks are created at the end close to the focus, and they move toward the microwave source. However the density peaks cannot move beyond a certain point in the system because the field strength is below the threshold beyond it. Asymptotic absorption is also obtained in this geometry, however, it increases with system length and beam convergence.

In all planar and spherical calculations, the electron temperature tends to be roughly 2 eV in steady state since the microwave strength is roughly the breakdown strength.

We have also simulated the recent focused microwave experiments[2] by two connected regions with different spherical convergence with and without a reflector at the focus. The ionization occurs initially near the focus, however the plasma grows much denser near the threshold region at later time and decouples the microwaves from the focal region. The length, location and motion of the plasma density profiles are in excellent agreement with those of the experiments.

The organization of this report is as follows. The Boltzmann equation is used and reduced to the proper kinetic description for the problem in Section II. In Section III moment equations are obtained for the problem with coefficients based on existing experimental data. Arguments are made to relate the data to the microwave field strength. In Section IV the experimental data and their range of validity are reviewed. Reflection and absorption of microwaves in the presence of plasma, treated both analytically and numerically, are given in Sections V and VI respectively. In Sections VII and VIII, microwave propagation, including the self-consistent hydrodynamics of the plasma, is investigated in both planar and spherical geometries. Hydrodynamic simulations of recent focused microwave experiments are described in Section IX. The work is summarized in Section X.

II. DESCRIPTION BY THE BOLTZMANN EQUATION

The kinetic theory of the electrons provides the essential description of the microwave-atmospheric interactions. The high-frequency phenomena associated with the motion of the ions and neutrals are insignificant due to much higher masses. Although any macroscopic measurement is an average of one sort or another, the microscopic description forms the basis for the understanding of the measurements. The treatment of the electron distribution f is described by the Boltzmann equation which is given by

$$\frac{\partial f}{\partial t} + \vec{v} \cdot \nabla f + \vec{a} \cdot \nabla_v f = C \qquad (1)$$

where $\vec{v}$ and $\vec{a}$ are the velocity and acceleration. The collisional term C represents the change of the distribution by elastic and inelastic collisional processes. Elastic collisions mainly result in the transfer of momentum and inelastic collisions are due to the excitation, ionization and attachment of the electrons.

The process of simplifying the Boltzmann equation can be based upon the high collisionality of the phenomena, especially in the lower atmosphere. For the less collisional higher atmosphere, the limitations of the description should be carefully justified. Since collisions take place in times of

order of 10^{-13} second (see Section IV) in the lower atmosphere, we assume that any substantial ordering of the direction of the motion of the electrons is prevented in the frequency range considered, and the velocity distribution is nearly spherically symmetrical at any point in space. Under this consideration, the electron distribution can be described in spherical expansions[3]

$$f = f_o + \hat{v} \cdot \vec{f}_1 + \hat{v}\hat{v} : \vec{\vec{f}}_2 \qquad (2)$$

where f_o represents the spherically symmetric part, and the $\vec{f}_1$ and $\vec{\vec{f}}_2$ represent the first and second order deviations from spherical symmetry, and $\hat{v}$ is the unit velocity vector. Similar to that for the distribution function, the expansion for the collision term is

$$C = C_o + \hat{v} \cdot \vec{C}_1 + \hat{v}\hat{v} : \vec{\vec{C}}_2 \qquad (3)$$

By substituting the expansions for f and C in the Boltzmann equation, we readily obtain the isotropic portion of the equation which is given by[3]

$$\frac{\partial f_o}{\partial t} + \frac{1}{3} v \nabla \cdot \vec{f}_1 + \frac{1}{3v^2} \frac{d}{dv} (v^2 \vec{a}_E \cdot \vec{f}_1) = C_o \qquad (4)$$

here $\vec{a}_E$ is the acceleration due to the electric field. And the first order anisotropic portion of the equation is given

by[3]

$$\frac{\partial \vec{f}_1}{\partial t} + v \nabla f_o + \vec{a}_E \frac{df_o}{dv} + \vec{a}_B \times \vec{f}_1 + \frac{2}{5} v \nabla \cdot \vec{\vec{f}}_2 + \frac{2}{5v^3} \frac{d}{dv} (v \vec{a}_E \cdot \vec{\vec{f}}_2) = \vec{C}_1 \tag{5}$$

here $\vec{a}_B$ is the acceleration due to the magnetic field.

Physically Eq. (4) determines the balance of the number density and energy of the electrons. Therefore the collision term C_o can be related to the distribution f_o by taking account of all elastic and inelastic collision processes. The elastic collision term should have the same form as that of the third term in equation (4) because it conserves particles. Therefore we have[3]

$$C_o = \frac{1}{v^2} \frac{d}{dv} (v^2 A(v) f_o) - \nu_s f_o \tag{6}$$

where: $A(v)$ is a function of v that is determined for elastic collisions of electrons with the heavier ions and neutrals. The second term contains ν_s which relates to the rates of excitation, ionization and attachment of electrons.

Eq. (5) determines the balance of the electron momentum. Therefore the collision term $\vec{C}_1$ can be related to the electron-neutral momentum transfer collision frequency ν_m as follows

$$\vec{C}_1 = -\nu_m \vec{f}_1 \tag{7}$$

Although Eqs. (4) and (5) describe only the zeroth and the first order distributions of the spherical expansion, they are exact even for an infinite spherical expansion[3]. For less collisional phenomena, in which the ordering expansion fails, Eqs. (4) and (5) still apply if the phenomena still fits the description of the definition of the distribution given by Eq. (2). Right now there is no ordering among $\vec{f}_o$, $\vec{f}_1$ and $\vec{\vec{f}}_2$. For both collisional and collisionless phenomena, $\vec{\vec{f}}_2$ can be modeled physically to close Eqs. (4) and (5).

For the problem of interest, we assume f_o represents only the low frequency response of the electrons. This is the same as assuming that high frequency charge separation does not occur. We also assume $\vec{\vec{f}}_2$ is only the low frequency response of the electrons due to the existence of the high frequency microwaves, that is the ponderomotive effect . Finally the high frequency response due to the microwaves enters only in

$\vec{f}_1$, therefore we set

$$\vec{f}_1 = \vec{f}_1^{\,h} e^{i\omega t} + \vec{f}_1^{\,L} \tag{8}$$

here the superscripts h and L represent the high and low frequency responses.

Substituting the high frequency part of Eq. (8) into Eq. (5) and assuming there is no dc magnetic field, we obtain a linearized high frequency equation as follows

$$\vec{f}_1^{\,h} = - \frac{\vec{a}_E^{\,h}}{(i\omega + \nu_m)} \frac{df_o}{dv} \tag{9}$$

For the low frequency part, Eq. (5) gives

$$\frac{\partial \vec{f}_1^{\,L}}{\partial t} + v \nabla f_o + \vec{a}_E^{\,L} \frac{df_o}{dv} + \frac{2}{5} v \nabla \cdot \vec{f}_2 = -\nu_m \vec{f}_1^{\,L} \tag{10}$$

We have neglected the second to last term in Eq. (5) in the above equations because this term is small and it actually does not contribute in the later equations.

III. MOMENT EQUATIONS FROM THE BOLTZMANN EQUATION

The macroscopic equations can be deduced from the kinetic equations described in Section II. Quite often we need to refer back to the kinetic theory in order to understand certain macroscopic measurements. For high frequency phenomena, we also need an equation, obtained from Faraday's and Ampere's laws of Maxwell equations, to describe the high frequency electric field $\vec{E}_h$

$$\frac{\partial^2}{\partial t^2} \vec{E}_h - c^2 \nabla^2 \vec{E}_h = 4\pi e \frac{\partial}{\partial t} \int \vec{v} f \, d\vec{v} \tag{11}$$

Here we have set $\nabla \cdot \vec{E}_h = 0$ since high frequency charge separation is neglected as described in Section II.

Substituting Eq. (9) into Eq. (11), the equation for microwave propagation is obtained, with $\vec{E}_h \propto e^{i\omega t}$, as follows

$$\nabla^2 \vec{E}_h + k_o^2 \, \varepsilon \, \vec{E}_h = 0 \tag{12}$$

here the complex dielectric function ε is given by

$$\varepsilon = 1 - \frac{4\pi e^2}{3m} \int f_o \frac{1}{v^2} \frac{d}{dv} \left(\frac{v^3}{\omega - i\nu_m}\right) d\vec{v} \tag{13}$$

In general ν_m is a strong function of v, therefore Eq. (13) is difficult to evaluate. However we will use Eq. (13) as a

definition for an effective high frequency collision coefficient ν_h as

$$\frac{1}{\omega - i\nu_h} = \frac{1}{3n} \int f_o \frac{1}{v^2} \frac{d}{dv} \left(\frac{v^3}{\omega - i\nu_m}\right) d\vec{v} \tag{14}$$

here $n = \int f_o \, d\vec{v}$. Notice that when the electron-neutral momentum transfer collision frequency ν_m is not a function of v, then $\nu_h = \nu_m$.

Using Eq. (4), the particle conservation equation can be obtained, after integrating over all velocity space, as follows

$$\frac{\partial n}{\partial t} + \nabla \cdot \vec{J} = - \int \nu_s f_o \, d\vec{v} \tag{15}$$

here $\vec{J} = 1/3 \int v \vec{f}_1^{\,L} \, d\vec{v}$. The source term is due to ionization and attachment of electrons.

The momentum conservation equation can be obtained from Eq. (5), after multiplying by mv/3 and integrating over all velocity space, and it is given by

$$m \frac{\partial \vec{J}}{\partial t} + \nabla p + en \vec{E}_L + \nabla \cdot \vec{\vec{p}}_2 = - \frac{m}{3} \int \nu_m v \vec{f}_1^{\,L} \, d\vec{v} \tag{16}$$

here m is the electron mass, $p = m/3 \int v^2 f_o \, d\vec{v}$, and $\vec{\vec{p}}_2 = 2m/15 \int v^2 \vec{\vec{f}}_2 \, d\vec{v}$. Here $\vec{\vec{p}}_2$ is the ponderomotive pressure tensor, which cannot be obtained in our present derivation, however, it can be derived using other approaches[4]. It is

given by[4]

$$\nabla \cdot \vec{P}_2 = \frac{mn}{4} \left(\nabla |\vec{u}_h|^2 - \frac{2}{\omega} \mathrm{Im} \left[\vec{u}_h \times \nabla \times (\nu_h \vec{u}_h^*) \right] \right) \qquad (17)$$

where $\vec{u}_h = 1/3n \int v \vec{f}_1^h \, d\vec{v}$, which is the high frequency oscillation velocity of the electrons due to the microwaves. The second term on the right hand side of Eq. (17) can be larger than the first term if $\nu_h >> \omega$. The first term prevails in the presence of substantial standing microwaves.

Basically we are more interested in the later time development of the phenomena, especially as the system approaches steady state. After the atmosphere is subjected to microwave breakdown, electrons and ions are created rapidly. As soon as a significant number of ions are created, the motion of the electrons is limited by the heavier ions through ambipolar drag. Therefore we set $\vec{j} = n\vec{u}$, here $\vec{u}$ is the hydrodynamic flow velocity of the ions. Because the ions do not interact with the microwaves the hydrodynamic description for the ions is appropriate. The momentum equation is given by

$$M\left(\frac{\partial}{\partial t} n\vec{u} + \nabla \cdot n\vec{u}\vec{u}\right) - en \vec{E}_L = 0 \qquad (18)$$

here M is the ion mass, and the ion-neutral collision and the thermal pressure of the ions have been neglected.

Combining Eqs. (16) and (18), $\vec{E}_L$ can be eliminated and

we obtain

$$M\left(\frac{\partial}{\partial t} n\vec{u} + \nabla \cdot n\vec{u}\vec{u}\right) + \nabla \cdot \vec{\vec{p}}_2 + \nabla p + \frac{m}{3} \int \nu_m v \vec{f}_1^{\,L} \, d\vec{v} = 0 \quad (19)$$

The evaluation of the last two terms comes from the experimental measurements which are usually done in the steady state and in absence of microwaves. In this case, a moment equation obtained from Eq. (10) is given by

$$\vec{j} = -\frac{e}{m} \vec{E}_A \int f_o \frac{1}{3v^2} \frac{d}{dv} \left(\frac{v^3}{\nu_m}\right) d\vec{v} - \frac{1}{3} \nabla \int f_o \frac{v^2}{\nu_m} d\vec{v} \quad (20)$$

The first term on the right hand side of Eq. (20) is the mobility term, and the second term is the diffusion term. The so-called swarm experiments[5-8] actually determined the drift and the ratio of the diffusion coefficient to the drift independently as functions of an applied electric field $\vec{E}_A$. Therefore an effective electron temperature can be defined as

$$\varepsilon_e = m \int f_o \frac{v^2}{\nu_m} d\vec{v} \Big/ \int f_o \frac{1}{v^2} \frac{d}{dv} \left(\frac{v^3}{\nu_m}\right) d\vec{v} \quad (21)$$

as a function of $\vec{E}_A$. Also an effective dc collision frequency ν_L can be defined as

$$\frac{1}{\nu_L} = \frac{1}{3n} \int f_o \frac{1}{v^2} \frac{d}{dv} \left(\frac{v^3}{\nu_m}\right) d\vec{v} \quad (22)$$

as a function of $\vec{E}_A$.

The best way to approximate the last two terms of Eq. (19) is to relate them to the above two defined quantities measured in the experiments, and Eq. (19) become

$$M\left(\frac{\partial}{\partial t} n\vec{u} + \nabla \cdot n\vec{u}\vec{u}\right) + \nabla \cdot \vec{\vec{p}}_2 + \nabla n\varepsilon_e + m\nu_L n\vec{u} = 0 \qquad (23)$$

here $\vec{\vec{p}}_2$ is given by Eq. (17) in term of $\vec{u}_h$, which can be derived from Eq. (9) to be

$$\vec{u}_h = -\frac{e}{m} \frac{\vec{E}_h}{(i\omega + \nu_h)} \qquad (24)$$

The independent variable $\vec{E}_A$ of ε_e and ν_L can be set to be equal to the microwave electric field as[1] (also see Section I)

$$\vec{E}_A = \frac{\vec{E}_h}{\sqrt{1 + \omega^2/\nu_h^2}} \qquad (25)$$

which is known as the effective electric field. The meaning of Eq. (25) is that $\vec{E}_A$ results in the same amount of collisional energy dissipation in both dc and ac cases, therefore it gives roughly the same ε_e and ν_L.

Also ν_h can be approximated by ν_L, especially in the highly collisional case. Since ν_h is also a function of $\vec{E}_h$, and so we see that the wave equation Eq. (12) is a nonlinear equation.

Finally the continuity equation Eq. (15) can be written as

$$\frac{\partial n}{\partial t} + \nabla \cdot n\vec{u} = (\nu_i - \nu_a)n \tag{26}$$

here ν_i and ν_a are the ionization and attachement rate coefficients. Both were measured in dc experiments[9-13] as functions of the dc electric field, which can be related to the microwave field defined in Eq. (25) using the above argument.

IV. RATE COEFFICIENTS FROM EXPERIMENTS

In order to investigate the dynamics of microwave breakdown in air, experimentally determined rate coefficients are required. Most of the measurements were done in dc experiments. However, there are ac experiments[1] which show that the breakdown thresholds of air is similar to that of dc experiments at high pressures. Within the accuracy (10-20%) of the experiments, several approximate formulae are modeled from various measurements for the rate coefficients. It turns out they can be described macroscopically, without knowing the details of their electron velocity dependence, by the microwave field strength.

The electron-neutral elastic collision frequency $\nu_c = \nu_h \approx \nu_L$ defined by Eqs. (14) and (22) is given by[5,6]

$$\frac{\nu_c}{p_{Torr}} = 5 \times 10^9 \sqrt{\frac{\alpha}{\alpha + 8}} \qquad (27)$$

in the range $0 < \alpha < 100$. Here α is a quantity related to the effective electric field described in Section III and is given by

$$\alpha = \frac{E_{rms}}{p_{Torr} \sqrt{1 + \omega^2/\nu_c^2}} \qquad (28)$$

Notice that Eq. (27) is a nonlinear equation for ν_c, and is roughly constant at high field.

Once the electrons are heated by the microwaves, the processes of excitation, ionization, and exchanging energy with the ions and neutrals occur. Energy balance on the collisional time scale will determine the electron temperature locally. The use of the measured temperature includes the electron energy gain and loss, and so an electron energy equation is not required. The electron temperature defined by Eq. (21) is given by[7,8]

$$\varepsilon_e^3 = 2.1 \times 10^{-3} \alpha (91 + \alpha) \qquad (29)$$

in the range $0 < \alpha < 40$, and ε_e is in eV. The temperature is a weak function of α as expected since the ionization and excitation restrict the energetic electrons. Even though the range is not large we an extrapolate to larger α because of the weak dependence on α.

Ionization occurs only when the microwave breakdown strength is reached, which is roughly[1] $\alpha \approx 32$. The ionization rate is given by[9,10]

$$\frac{\nu_i}{p_{Torr}} = 5.14 \times 10^{11} \exp(-73\, \alpha^{-0.44}) \qquad (30)$$

in the range $32 < \alpha < 100$.

Attachment occurs due to the combination of electrons with the neutrals. In our case, two processes ($e + O_2$) and ($e + 2O_2$) can be dominant. The two-body attachment rate is given by[11-13]

$$\frac{\nu_{a2}}{p_{Torr}} = 7.6 \times 10^{-4} \alpha^2(\alpha + 218)^2 \tag{31}$$

in the range $0 < \alpha < 60$ and the three-body attachment rate is given by[13]

$$\frac{\nu_{a3}}{p_{Torr}} = 5.7 \times 10^5 \, p_{atm} \frac{\alpha^{1/3}}{\alpha + 6.1\,\alpha^{2/3} + 1.6\,\alpha^{1/3} + 0.11} \tag{32}$$

in the range $0 < \alpha < 5$ which corresponds to $0 < \varepsilon_e < 1$ eV. Notice that ν_{a3} is only important at very low microwave strengths. Also ν_{a2} is not important as compared to the ionization rate for larger values of α after the breakdown.

V. REFLECTION OF MICROWAVES BY FIXED ELECTRON DENSITY PROFILES

The reflection of microwaves by the breakdown plasma in the atmosphere is a key factor in the determination of how much microwave power can be delivered through the atmosphere. Here we will calculate the reflection of the microwaves for various electron density profles. We find that the reflection basically depends on the height and the slope of the density. Both analytical and numerical calculations will be presented.

The one-dimensional wave equation (from Eq. 12) can be written as (for simplicity the subscript is dropped)

$$\frac{d^2E}{dx^2} + k_o^2 \varepsilon E = 0, \quad \varepsilon = 1 - \frac{n}{n_c(1 - i\nu_c/\omega)} \tag{33}$$

Since ν_c, given by Eqs. (27) and (28), is a function of E, therefore the wave equation is a nonlinear equation of E.

When the reflection is very weak, ν_c can be considered as a constant in space where E is quite constant along the reflection path. In this case we actually can analytically solve Eq. (33). Two types of plasma density profiles are consiered. The first type is an exponential density profile which is given by

$$\frac{n}{n_c} = \exp(x/\ell) \tag{34}$$

The second type is a linear density profile which is given by

$$\frac{n}{n_c} = \frac{x}{L} \qquad \text{for } x > 0 \tag{35}$$

Notice that $\ell = n(dn/dx)^{-1} = L\, n/n_c$ is the local density gradient scale length for both profiles.

The reflection can be obtained analytically for constant ν_c for the above density profiles by using the Phase-Integral Method[14]. The reflection of wave energy is given by

$$R = \left| \exp\left(2ik_o \int_{-\infty}^{z_o} \sqrt{\epsilon}\, dz\right)\right|^2 \tag{36}$$

here z_o is the complex point where the complex dielectric function $\epsilon = 0$. For an exponential profile Eq. (35) becomes[14]

$$R = e^{-4\, k_o \ell \tan^{-1}(\nu_c/\omega)} \tag{37}$$

and for a linear profile it is given by[14]

$$R = e^{-\frac{8}{3} k_o L\, \nu_c/\omega} \tag{38}$$

From Eqs. (37) and (38), it can concluded that reflection is important when

$$k_o \ell \tan^{-1}(\nu_c/\omega) < 1 \tag{39}$$

and

$$k_o L\, \nu_c/\omega = k_o \ell \frac{n_c}{n} \frac{\nu_c}{\omega} < 1 \tag{40}$$

In fact, Eq. (40), which is for a linear profile, is roughly the same as Eq. (39) if we use the turning point density ($\varepsilon = 0$) in Eq. (40). From Eq. (33), the turning point density roughly is

$$\frac{n_t}{n_c} = (1 + \nu_c^2/\omega^2)^{1/2} \tag{41}$$

Using the turning point density in Eq. (40), we find,

$$k_o \ell \, \nu_c/\omega \, (1 + \nu_c^2/\omega^2)^{-1/2} < 1 \tag{42}$$

One can see that Eqs. (39) and (42) are roughly comparable.

In general Eq. (39) and $n > n_t$ can be considered to be the conditions that reflection becomes important. In the limit $\nu_c/\omega >> 1$, they are given by

$$k_o \ell < 1 \quad \text{and} \quad n > n_c \nu_c/\omega \tag{43}$$

and in the limit $\nu_c/\omega << 1$, they are given by

$$k_o \ell < \omega/\nu_c \quad \text{and} \quad n > n_c \tag{44}$$

In useful atmospheric units, the two conditions can be rewritten roughly (valid for $P_{atm} > 10^{-3} f_{GHz}$) as

$$\ell(\text{cm}) < f^{-1}_{GHz} \text{ and } n(\text{cm}^{-3}) > 10^{13} P_{atm} f_{GHz} \tag{45}$$

and (valid for $P_{atm} < 10^{-3} f_{GHz}$) as

$$\ell(\text{cm}) < 10^{-2} P_{atm}^{-1} \text{ and } n(\text{cm}^{-3}) > 10^{10} f^2_{GHz} \tag{46}$$

From Eqs. (45) and (46), one can see that reflection is important at higher atmospheric altitude and lower microwave frequency.

The above analytical calculations are only valid for weak reflection. For a complete treatment of reflection, numerical calculations have to be made. Computations are made for a one-dimensional finite region. The boundary conditions are incoming and reflected microwaves at the left, and transmitted microwaves at the right. Eq. (33) is solved with $\nu_c(E)$ by iteration. The coefficients of reflection, absorption and transmission are measured at the boundaries.

The numerical solution in Figure 1 shows the portion of microwave energy reflected just before reaching a point on the density profile as a function of the local density at that point for various values of ℓ and L. The calculation is done in very collisional air ($\nu_c/\omega \sim 10^2$) with p = 1 atm, f = 3.2 GHz, and $E_{rms}/p_{Torr} = 40$. Obviously, a significant portion is reflected after $n/n_c < \nu_c/\omega$, which is the second condition of Eq. (43).

After the microwaves have passed a certain density, the reflection reaches its maximum value (Figure 1) which is a function of the density scale length. The density scale

length for the maximum value is shown in Figure 2. The results $k_o \ell < 1$ and $k_o L < 10^{-2}$ (therefore $k_o \ell = k_o L n/n_c < 1$ since $n/n_c \sim \nu_c/\omega \sim 10^2$) for reflection to be significant are just the same as the first condition of Eq. (43).

Results for the reflection as a function of atmospheric pressure (or equivalently as a function of microwave frequency) are presented in Figure 3. Other parameters are the same as previously. The value of ν_c/ω is roughly 10^2 P_{atm} in this case, therefore the region $P_{atm} < 10^{-2}$ corresponds to a less collisional atmosphere. In this region the turning point is approximately at n_c, corresponding to the second condition of Eq. (44). Also $L = \ell$, each $k_o \ell \geq 1$ curves for both profiles are quite similar to each other and they give the first condition of Eq. (44).

We have also calculated the dependence of reflection on the incoming microwave power. It was found that the dependence is very weak as long as $E_{rms}/P_{Torr} >> 8$, as can be seen in Eq. (27). This is the usual case in the microwave breakdown atmosphere.

VI. ABSORPTION OF MICROWAVES BY FIXED ELECTRON DENSITY PROFILES

In the previous section we have calculated the reflection of microwaves for fixed plasma density profiles. Similar calculations have been done for absorption. Without significant reflection, the absorption can be represented as a phase-integral[14] of a traveling wave which is given by

$$A = 1 - \left| \exp\left(-i\, k_o \int_o^x \sqrt{\epsilon}\, dx\right)\right|^2 \tag{47}$$

In general Eq. (47) is difficult to evaluate. Here we consider a simple case with a constant plasma density slab and constant collision frequency ν_c. The absorption, for weak reflection, is given by

$$A = 1 - \exp\left[-\frac{\nu_c}{\omega}\frac{n}{n_c} k_o \Delta / \sqrt{(1 + \nu_c^2/\omega^2)(1 + \nu_c^2/\omega^2 - n/n_c)}\right] \tag{48}$$

here Δ is the width of the slab. For the $\nu_c/\omega \gg 1$, the absorption is given by

$$A = 1 - \exp\left(-\, n/n_c\, \omega/\nu_c\, k_o \Delta\right) \tag{49}$$

The highly collisional case is more interesting because it gives high absorption. For comparison, numerical results (described in Section V) are plotted in Figure 4 for a plasma slab of width 1 and 5 λ_o, here λ_o is the microwave wavelength.

Other parameters are p = 1 atm, f = 3.2 GHz and E_{rms}/P_{Torr} = 40 (as is in Figure 1 in very collisional air). One can see that almost total absorption is obtained before the turning point density $n/n_c \sim 10^2$, where the reflection becomes significant. These portions of the absorption curves agree very well with Eq. (49) if we use an average, $\nu_c/\omega \sim 150$. At higher density, the absorption is reduced due to the increase in microwave reflection. However the reduction is less if other more gentle density profiles are used, since here the step profile gives the most severe reflection.

If the reflection is not serious, Eq. (49) shows that good absorption occurs for

$$\frac{n}{n_c} k_o \Delta > \frac{\nu_c}{\omega} \tag{50}$$

Rewritten in atmospheric units, Eq. (50) becomes

$$n\ \Delta(cm^{-2}) > 10^{13}\ P_{atm} \tag{51}$$

Since the atmospheric density is N 3 x 10^{19} P_{atm} cm^{03}, therefore Eq. (51) becomes

$$\frac{n}{N}\ \Delta(cm) > 10^{-6} \tag{52}$$

For plasma slabs of width on the order of centimeters, a small percentage of ionization gives good absorption.

Although only a constant plasma density slab is used here for absorption calculations, other density profiles will give similar results with an effective width Δ to be defined as the full half-width of the profile. We have proved this numerically.

VII. MICROWAVE ABSORPTION WITH HYDRODYNAMICS IN PLANAR GEOMETRY

All the previous calculations of reflection, absorption and transmission coefficients use only fixed plasma density profiles. In a realistic situation, the density profile should be determined self-consistently with the microwaves. The time evolution of the density profile was derived in Section III, and the one-dimensional continuity and momentum equations are given by Eqs. (26) and (23) as follows

$$\frac{\partial n}{\partial t} + \frac{\partial}{\partial x}(nu) = (\nu_i - \nu_a)\, n \tag{53}$$

and

$$M\left(\frac{\partial}{\partial t} u + u \frac{\partial}{\partial x} u\right) + \frac{1}{n}\frac{\partial}{\partial x} n \varepsilon_e + f_p + m\nu_c u + M(\nu_i - \nu_a)u = 0 \tag{54}$$

where f_p is the ponderomotive term which is given by

$$f_p = \frac{m}{4}\left[\frac{\partial}{\partial x}|u_h|^2 - 2\frac{\nu_c}{\omega} Im\left(u_h \frac{\partial}{\partial x} u_h^*\right)\right] \tag{55}$$

All the rate coefficients ν_i, ν_a, ν_c and ε_e are functions of E as described in Section IV. Consequently the hydrodynamics of the system evolves according to the microwave fields (Eq. 33).

Without any pre-arrangment, the electron density usually grows in all space evenly from noise once the microwave power is above the breakdown threshold. After some time, the densi-

ty even grows faster at the places closer to the microwave source because the microwaves are stronger there due to reflection. Finally the microwaves will be cut-off due to the very high plasma density near the source. This is not the case of interest because after a while the microwaves are blocked from leaving the source.

The important issue is how the system can be designed to achieve the desired physical result. Two cases will be investigated here. First, a local region is pre-ionized by other means, and second a reflector is placed in the system. The two cases will be examined separately in the following subsections.

A. Pre-ionized Localized Plasma Density

If we initialize the plasma in a very narrow region of relatively high density, then the plasma grows to high enough density to cause high absorption before the density at other places grows significantly. Hopefully, enough energy could be absorbed in the time interval before the plasma grows in the regions that are not pre-ionized. The pre-ionization could be produced by other devices.

We will start with strongly collisional cases. The first calculation is shown in Figure 5 with $E_{rms}/P_{Torr} = 40$ ($I = 2.5$ MW/cm^2), $p = 1$ atm, $f = 3.2$ GHz, and an initially localized plasma density $n/n_c = 1$ ($n \sim 10^{11}$ cm^{-3}) at $k_o x = 14$ and $n/n_c = 10^{-10}$ elsewhere. The position of the pre-ionized plasma is indicated by an arrow in the figure. The plasma density grows in time and moves toward the microwave source. Two density profiles at later times $t = 50$ nsec and 100 nsec are shown in the figure. This motion of the profile is mainly due to the ionization process by the larger microwave field in front and the de-ionization process by the smaller field at the back of the profile.

Roughly starting from $t = 100$ nsec, the density profile evolves very slowly toward steady state with the incoming mi-

crowaves. The asymtotic behavior of this sort can be seen in the time history of the absorption as shown in Figure 6. The asymptotic maximum density is $n_{max}/n_c \sim 60$ and the asymptotic absorption is about 0.82 with little reflection. The small reflection is consistent with the prediction in Section V (here $\nu_c/\omega \sim 10^2$). At t ~ 200 nsec, the asymtotic density profile is destroyed due to density growth evolved at locations other than the preionized region.

The motion toward the source is very rapid. The speed is about 10^8 cm/sec, which is 2 or 3 orders higher than the sound speed. Therefore it is due to the rapid ionization rate. The front slope, roughly represented by an exponential profile with $k_o \ell \sim 1$, remains about the same for all time.

We have tried to find how the initial pre-ionization affects the asymptotic results. It turns out that the product of the maximum and the width of the asymptotic density profile and the absorption remain about the same. The first line in Table 1 (a) shows the results for the case we just described, and the results for an identical case but with a different initial pre-ionization are given in the second line. The same thing happens when the frequency is varied as shown in line 3 in Table 1 (a). All cases give the roughly same $n\Delta$ such that the value of $\frac{n}{n_c} \frac{\omega}{\nu_c} k_o \Delta$ in Eq. (49) is found to be roughly the

same and therefore the absorption is the same.

The above constant absorption phenomena, for the same microwave power and atmospheric pressure, can be explained as follows. Near the peak of the density profile, the microwave field strength has to be near $E_{BD} \sim 32\ P_{Torr}$ which is the breakdown threshold, so that steady state is achieved. The required attenuation of the incoming microwave field to E_{BD} fixes the value of $n\Delta$. Therefore fixed absorption is achieved by varying either the maximum or the width of the density profile. This is just what has been seen in the hydrodynamic calculations.

For higher microwave power, more absorption is required to attenuate the microwave field strength to E_{BD}. Therefore higher absorption results for higher power. In Table 1 (b) absorption is listed for various microwave powers. One should note that absorption increases rapidly until the microwaves are totally absorbed. If the microwave power is fixed, absorption decreases with the atmospheric pressure. The dependency goes roughly with the effective microwave strength $\alpha \approx E_{rms}/P_{Torr}$.

We also find that the density required for significant reflection (Eq. (43)) is not attained therefore there is

little reflection, and that the density scale length $k_o \ell$ does not vary very much in general because the microwave strength is attenuated to $\alpha \approx 32$ at steady state.

Now we turn to weakly collisional cases. Since the conditions $k_o \ell < \omega/\nu_c$ and $n > n_c$ (Eq. 44) are easier to meet, here reflection dictates the microwave absorption. As before the value of $k_o \ell$ does not vary very much at steady state, therefore the reflection depends mainly upon ν_c/ω (Eq. 37) or the collisionality of the system.

The parameters used in the hydrodynamic calcalations in the weakly collisional cases are typically I = 33 kW/cm^2 (E_{rms} = 3500 volt/cm), f = 35 GHz, and the initial pre-ionized density is 0.1 n_c with width 0.25 λ_o. In this case $\nu_c/\omega \approx 17\ P_{atm}$. The calculations show that, as in the collisional cases, the plasma density front moves toward the microwave source and reaches steady state, however the profile at the back continues to be elongated due to the weak de-ionization rate there. Nevertheless the elongation does not affect the reflection in the front and the microwave energy that is not reflected will be absorbed.

Runs with various pressures (or collisionality) are shown in Figure 7 in which the weakly collisional regime is that for

which $p_{atm} << 0.1$. In Figure 7 (a), the asymptotic density height obtained in the weakly collisional regime is roughly constant since $\alpha \approx 0.783\ E_{rms}/f_{GHz}$ does not depend upon pressure. Also the asymtotic absorption increases (reflection decreases) with pressure as predicted in the previous discussion. The cutoff at $P_{atm} \geq 0.13$ is due to $\alpha \leq 32$ so that the power is below the breakdown threshold. The speed of the ionization front toward the microwave source is shown in Figure 7 (b).

B. Reflector at the Boundary

If a reflector is put at the right boundary, standing microwaves will be formed. The incoming power is below the breakdown threshold, therefore the problem of cutting off the microwaves near the source mentioned above can be avoided. However the maxima of the standing wave can be above the breakdown threshold, so that plasma is generated resulting in absorption.

A collisional case (Figure 8) with $E_{rms}/P_{Torr} = 20$ ($I = 0.62$ MW/cm^2), P = 1 atm and f = 3.2 GHz is run for a system of length, $L = 3.1\ \lambda_o$. Here the incoming wave $\alpha = 20$ is below breakdown threshold, however the standing wave $\alpha = 40$ is well above threshold.

Roughly starting from time t = 100 nsec, the density profile evolves very slowly towards stationary steady state. Figure 8 shows the asymptotic microwave and density profiles at t = 200 nsec. One can see that the density profile forms with spikes aligned with the anti-nodes of the standing wave. The absorption at this time is about 57% such that the maxima of the standing wave no longer is $\alpha \simeq 40$ but $\alpha \simeq 32$, which is the breakdown threshold, so that a steady state is achieved.

Calculations also have been performed for $L = 1.5\ \lambda_o$ and $6.2\ \lambda_o$. The asymtotic results for the three cases are listed in Table 2 (a). One can see that the product of the length of the system and the maximum density for each case are roughly the same, so that the absorption is roughly the same (Eq. 49). This is the same constant absorption phenomenon discussed in the previous subsection. In this case, the absorbed energy is distributed among the density spikes. If there are a large number of density spikes, the maximum density in each spike is smaller.

As in the last subsection, the absorption increases as the power increases. This is listed in Table 2 (b), showing the values of the absorption and the power. Near the breakdown threshold, the microwaves are completely absorbed.

The advantage of the case with reflector is that there is absorption of the microwaves in the stationary state. Whereas in the previous case with pre-ionization the moving steady state stays only for a finite time.

VIII. MICROWAVE ABSORPTION WITH HYDRODYNAMICS IN SPHERICAL GEOMETRY

The problem of cutting-off the microwaves near the source can be avoided by using converging microwave beams that are above breakdown threshold only near the focal region. The convergence of the microwaves can be obtained from structured or several antennas, or just due to the self-focusing of the microwaves. The actual geometry can be very complicated, for simplicity, here we use spherical geometry to simulate these effects. We assume that all the quantities are functions of r, the spherical coordinate, only. For normally incident microwaves, assuming $k_o r \gg 1$, Eq. (12) can be written as[15]

$$\frac{d^2}{dr^2} E + \frac{2}{r} \frac{d}{dr} E + k_o^2 \varepsilon E = 0 \qquad (56)$$

Assuming the velocity of the flow is in r-direction only, then the continuity equation (Eq. 26) becomes

$$\frac{\partial n}{\partial t} + \frac{1}{r^2} \frac{\partial}{\partial r} (r^2 \, nu) = (\nu_i - \nu_a) n \qquad (57)$$

The momentum equation is the same as Eq. (54) in the previous section with x replaced by r.

We have run a case with $E_{rms}/P_{Torr} = 30$ ($I = 1.45$ MW/cm^2 which is just below breakdown threshold), p = 1 atm and

f = 3.2 GHz in a system that extends from k r = 80 to k r = 100. The initial plasma density is n/n_c = 1 everywhere (this does not affect the later stage). The density and microwave profiles are shown in Figure 9 at time t = 100 and 500 nsec respectively. The density grows initially at the far right until transmission of the microwaves is blocked to a value just below the breakdown threshold. The density peak grows to $n/n_c \sim 7$ and moves toward the microwave source. At t = 500 nsec the density peak moves very close and slowly to the source such that the transmitted microwaves pick up some strength at the far right again to initialize another density peak. The process repeats itself. At this time the absorption oscillates about an asymptotic value of about 18% with little reflection.

Another system with $60 \leq k_o r \leq 100$, which is twice as long, has been run with the same parameters. Figure 10 shows the late time profiles at t = 1250 nsec. Many density peaks have emerged and move toward the source. The density peak cannot move beyond $k_o r = 90$ because the microwave strength is below the breakdown threshold to the right of that point. The microwaves in the system are attenuated to the breakdown value. The absorption oscillates about an asymptotic value of about 56% with little reflection.

In Table 3 the asymptotic absorption in systems of different lengths is listed. We see that the longer the system the higher the absorption, and absorption increases as the microwave convergence increases (line 4).

IX. SIMULATIONS OF FOCUSED MICROWAVE EXPERIMENTS

In the experiments[2] carried out at NRL (Figure 11), the microwaves (frequency 35 GHz and Power 112 kW) are focusd through a lens (7.6 cm diameter and 11.2 cm focal length) into the nitrogen gas (25 Torr). The measured elliptic area of the focus is π x 0.55 cm x 0.75 cm. Using a circular area to model the measured elliptic area, the equivalent radius is 0.64 cm. The radial profile of the microwaves is approximated by a Gaussian with an e-folding distance of 0.77 cm. The maximum power flux is 60 kW/cm (equivalent to the total power evenly distributed in a circle of radius 0.77 cm) at the axis.

The diffraction of the microwaves starts to occur at an axial distance of 3.5 cm (4 wavelengths) from the focus. Between this point and the lens, the microwaves are focused spherically. Our simulation starts at an axial distance of about 6 cm (7 wavelengths) from the focus with $I \approx 8.2$ kW/cm^2 at the axis (equivalent to the total power evenly distributed in a circle of radius 2.1 cm). The microwaves are focused spherically in a distance of 2.5 cm and connected to the solution in the diffraction region (3.5 → 0 cm). We approximate the diffraction effect by another spherical effect of aspect ratio 1.55 (equivalent to a 0.77 cm radius circle at focus and 1.2 cm radius circle at 3.5 cm). The schematic of

the simulation region is shown in Figure 11.

Although the coefficients in our computer code are for air, the code can be used to approximate N gas. As in the experiments, two cases are run with and without a metalic reflector placed at the focus. The microwave pulse length is 1 μsec.

In the case without reflector, the spatial profiles are presented in Figures 12 and 13 (microwaves incoming from the left). At t = 50 nsec, the ionization of the air by the microwaves occurs mainly near the focus (Figure 12 a), however, at the same time the microwaves are attenuated there due to the presence of the plasma (Figure 13 a). The associated electron temperature is plotted in Figure 13 (b).

At t = 100 nsec, the plasma grows faster near the connection region (Figure 12 b) because the microwaves are stronger there. At t = 400 nsec, the plasma at the ionization front reaches the collisionless critical density and becomes thicker (Figure 12 c), thus the microwaves are decoupled from the focal region. The ionization front moves slowly toward the microwave source until at t = 1 μsec (Figure 12 d), and the front cannot move beyond 6 cm because the microwave strength is below the breakdown threshold beyond that point. The de-

coupling of the microwaves from the focal region at 1 μsec is shown in Figure 13 (a).

The calculated profiles agree quite well with those from the experiments without a reflector (the frame pictures presented in Figure 2 of reference 2). The common observations are (1) the initial less dense plasma near the focal region, (2) the much denser plasma just inside the breakdown region at later times, (3) the slow motion of the denser plasma at later times, and (4) the length of the ionization region being about 5 cm.

Our calculated plasma density ($4 \times 10^{12} - 2 \times 10^{13}$ cm^{-3}) is also within the experimental measured range. However, our calculated electron temperature is roughly an eV lower. The higher experimental value is probably due to the use of 15 Torr N_2 and 19 Torr He at the time of the measurement of the electron temperature.

The calculated spatial profiles are presented in Figures 14 and 15 for the case of a metal reflector at the focus perpendicular to the incoming microwaves. Because of the standing waves set up by the reflector, the initial ionization is stronger and spatially more non-uniform than in the previous case. This is shown in Figure 14 (a) for an early time, t =

10 nsec. The standing wave characteristic is shown in Figure 15 (a) with the microwaves attenuated near the focus due to the presence of the plasma.

As in previous cases, the plasma grows faster near the connection region and moves out slowly as shown in Figure 14 (b), (c), and (d) at t = 100, 400 and 1000 nsec respectively. However, the denser plasma profile in this case is split due to the growth of the spikes. The decoupling of the microwaves from the focal region at t = 1 μsec is shown in Figure 15 (b).

Qualitatively the cases without and with reflector are similar. This is consistent with the observations in the experiment (Figures 2 and 3 in Reference 2 for the two cases). The additional features due to the presence of the reflector shown in the frame pictures are (1) stronger ionization in the focal region at early time and (2) the spiky feature. In general, similar results are obtained at later times due to the strong absorption ($A \geq 90\%$) of the microwaves by the plasma, such that the reflection by the reflector is not important.

The motion of the ionization front and the decoupling of the microwaves can be seen in the time plot of the position of the maximum of the electric field in Figure 16 (similar feature for the case without reflector). As quickly as 50

nsec, the microwaves are decoupled from the focal region. After that the ionization front moves slowly just inside the breakdown region. The speed of the ionization front is obviously a function of time. The average speed is 4 to 5 x 10^6 cm/sec. The time plots agrees with the experimental observations (Figure 3 b in Reference 2).

X. SUMMARY

In this report the air breakdown due to microwaves propagating in the atmosphere is investigated. The kinetic and hydrodynamic descriptions of the problem are reduced from the Boltzmann equation. The available experimental data for rate coefficients are used and related to the microwave field strength macroscopically. The important processes are electron-neutral collisions, ionization, attachment, and excitation. Thermal equilibrium of the electrons with the microwaves is also obtained.

Reflection and absorption of the microwaves in the presence of the plasma density profiles are investigated both analytically and numerically. Conditions for reflection and absorption are obtained.

Hydrodynamic calculations in planar geometry were carried out for two cases: pre-ionization in a locallized region initially and with a reflector at a boundary. In the first case, enough microwave energy can be absorbed in the time interval of interest, whereas a stationary state can be achieved in the second case. Calculations in spherical geometry show that many density peaks emerge from the end close to the focus and deccelerate toward the microwave source.

Some typical planar results show that the air is ionized rapidly to form an ionization front moving toward the microwave source which consequently decouples the microwaves from the original region. By focusing the microwaves or placing a reflector, localized regions can be heated by the microwaves.

The electron temperature obtained tends to be roughly 2 eV at steady state regardless of the microwave power. The heated electrons are able to exchange energy with the neutral atmospheric molecules[16] and will possibly enhance the neutral temperature.

At high altitude, the heating of electrons by other mechanisms, such as the collective plasma effects, is possible. Two effects, parametric instabilities[17] and resonant absorption[18], can result in heating suprathermal electrons with higher temperature. These effects are being investigated.

The limitations of the calculations are due to the availability of the experimental data for the rate coeffients. Nevertheless, comparison of the calculations with recent microwave experiments give excellent agreement. More accurate rate coefficients are being investigated[19] in the presence of a microwave discharge.

REFERENCES

1. A. D. MacDonald, D. U. Gaskell, and H. N. Gitterman, Phys. Rev. 5, 1841, (1963), and references therein.

2. W. M. Bollen, C. L. Yee, A. W. Ali, M. J. Nagurney, and M. E. Reed, J. Appl. Phys. 54, 101, (1983).

3. I. P. Shkarofsky, T. W. Johnston, and M. P. Bachynski, "The Particle Kinetics of Plasmas", Addison-Wesley, London, p. 70, (1966).

4. W. Woo, and J. S. DeGroot, Phys. Fluids 21, 124 (1978).

5. R. A. Nielsen and N. E. Bradbury, Phys. Rev. 51, 69, (1937).

6. H. Ryzko, Proc. Phys. Soc. 85, 1283 (1965).

7. R. W. Crompton, L. G. H. Huxley, and D. J. Sutton, Proc. Roy. Soc. A218, 507 (1953).

8. J. A. Rees and R. L. Jory, Aust. J. Phys. 17, 307 (1964).

9. J. Dutton, F. M. Harris and F. L. Jones, Proc. Phys. Soc. 81, 52, (1963).

10. M. J. Druyvesteyn and F. M. Penning, Rev. Mod. Phys. 12, 87, (1940).

11. P. A. Chatterton and J. D. Craggs, Proc. Phys. Soc. 85, 355, (1965).

12. M. A. Harrison and R. Geballe, Phys. Rev. 91, 1, (1953).

13. L. M. Chanin, A. V. Pleps, and M. A. Biondi, Phys. Rev. 128, 219 (1962).

14. J. Heading, "An Introduction to Phase Integral Methods", Wiley, New York, P. 81 (1962).

15. W. Woo, R. B. Spielman, and J. S. DeGroot, Bull. Am. Phys. Soc. 23, 792 (1978).

16. S. C. Lin, and G. P. Theofilos, Phys. Fluids 6, 1369 (1963).

17. K. Mizuno, and J. S. DeGroot, Phys. Rev. Lett. 35, 219 (1975).

18. K. Mizuno, J. S. DeGroot, and F. Kehl, Phys. Rev. Lett. 49, 1004 (1982).

19. G. August, private communication.

Table 1

(a) f (GHz)	n/n_c	Δ/λ_o	absorption
3.2	60	0.6	0.82
3.2	27	1.3	0.80
32.0	6	0.6	0.82

(b) E_{rms}/P_{Torr}	Power (MW/cm^2)	absorption
35	1.9	0.33
40	2.5	0.82
45	3.1	0.97
50	3.8	0.99
60	5.5	1.00

Asymptotic values of density height, width and microwave absorption from planar hydrodynamic calculations in very collisional air with pre-ionization. (a) Results obtained, lines 1 and 2, by varying initial pre-ionization and, lines 1 and 3, by varying frequency. They all give roughly the same $n\Delta$ and absorption. Here $p = 1$ atm and $I = 2.5$ MW/cm^2. (b) Absorption increases as power increases. Here $p = 1$ atm and $f = 3.2$ GHz.

Table 2

(a)

L/λ_o	n/n_c	absorption
1.5	44	0.60
3.1	19	0.57
6.2	11	0.62

(b)

E_{rms}/P_{Torr}	Power (MW/cm^2)	absorption
20	0.62	0.60
25	0.96	0.89
30	1.40	0.99

Asymptotic values of density height and microwave absorption from planar hydrodynamic calculations in very collisional air with reflector. (a) Results obtained by varying the system length. They all give roughly the same nL and absorption. Here p = 1 atm, f = 3.2 GHz and I = 0.62 MW/cm^2. (b) Absorption increases as power increases. Here p and f are the same as in (a).

Table 3

Region of computation	absorption
$80 \leq k_o r \leq 100$	0.18
$60 \leq k_o r \leq 100$	0.56
$40 \leq k_o r \leq 100$	0.80
$30 \leq k_o r \leq 50$	0.55

The asymptotic values of microwave absorption from spherical hydrodynamic calculations for systems of different lengths. The longer or the more convergent the system is the higher the absorption. Here p = 1 atm, f = 3.2 GHz and I = 1.45 MW/cm^2.

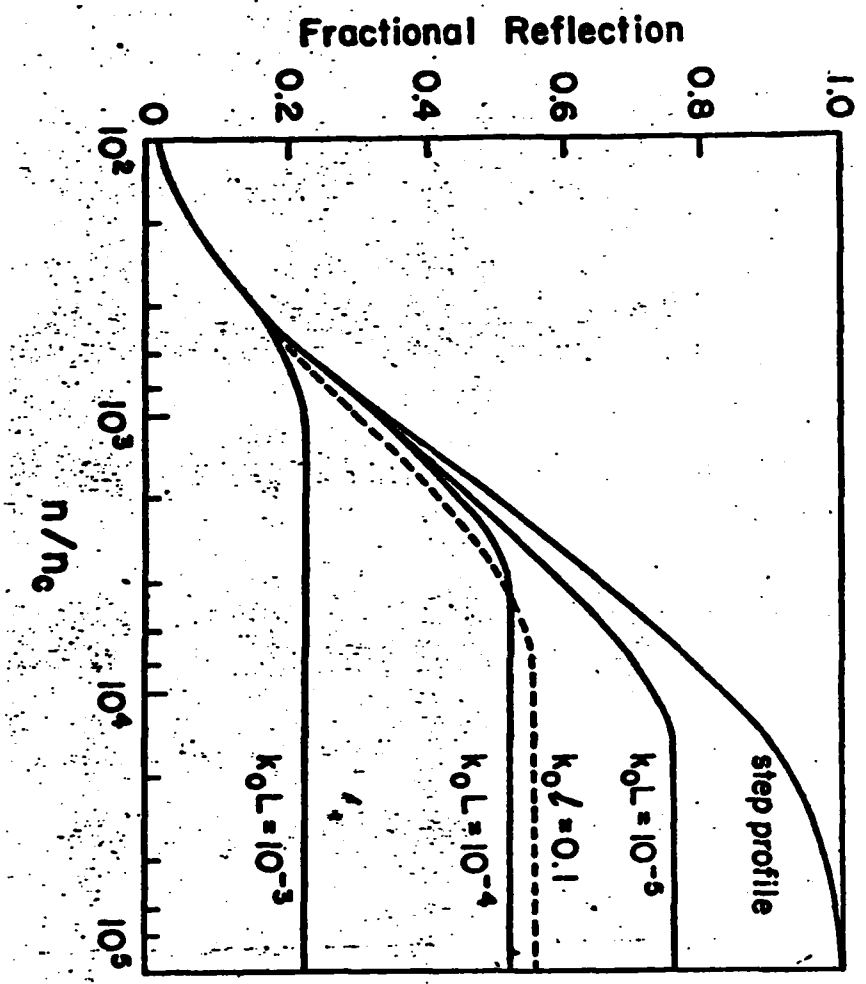

FIGURE 1

The portion of microwave energy reflected just before reaching a point on the plasma density profile as a function of the local density at that point. The curves are for exponential (with ℓ), linear (with L), or step profiles. The calculation is done in very collisional air with p = 1 atm, f = 3.2 GHz, and I = 2.5 MW/cm^2 (E_{rms}/p_{Torr} = 40).

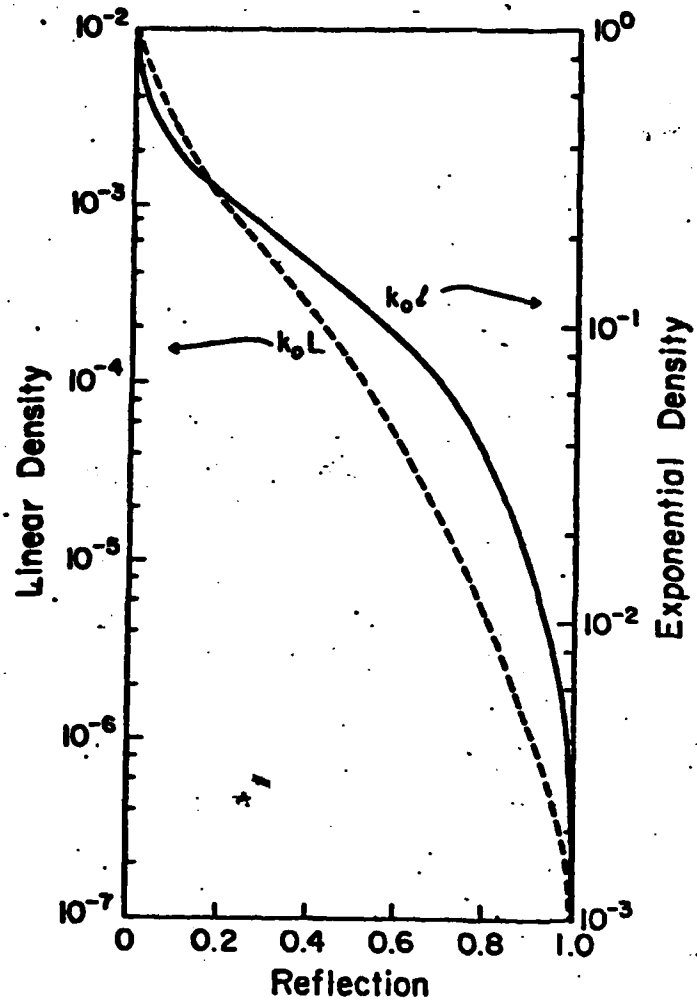

FIGURE 2

The maximum reflection from Figure 1 as a function of plasma density scale length.

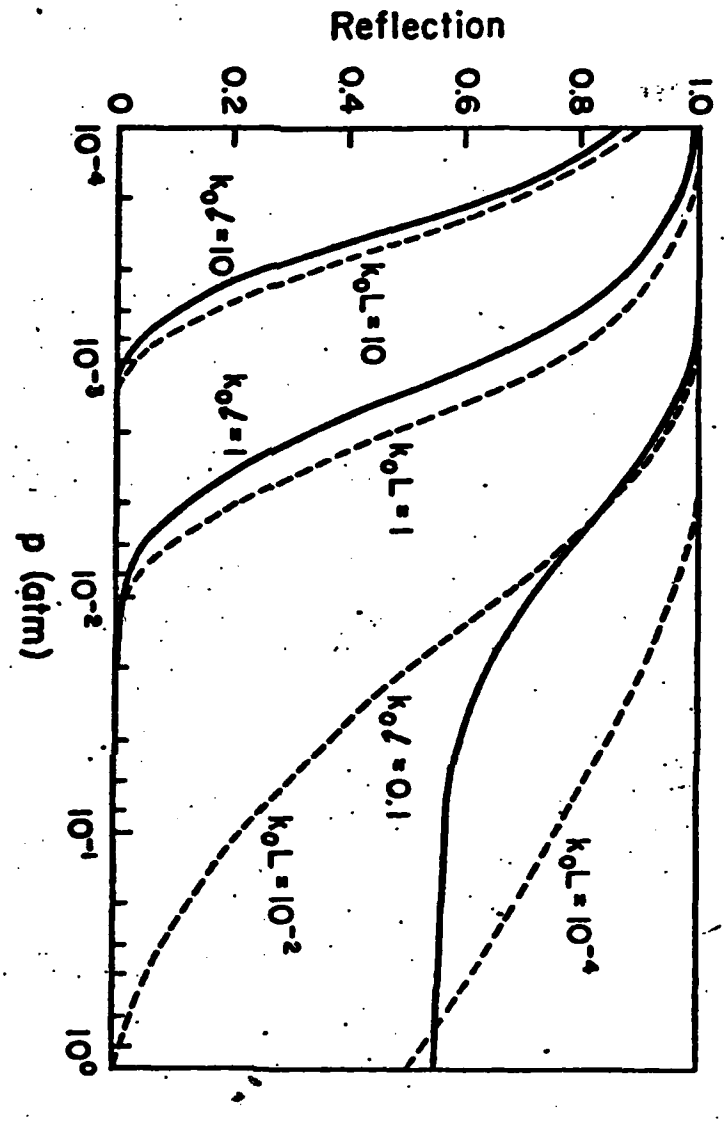

FIGURE 3

Reflection as a function of pressure for various plasma density scale lengths. This case has the same f and E/P as in Figure 1. The boundary between strong and weak collisionality is roughly at $p \sim 10^{-2}$ atm.

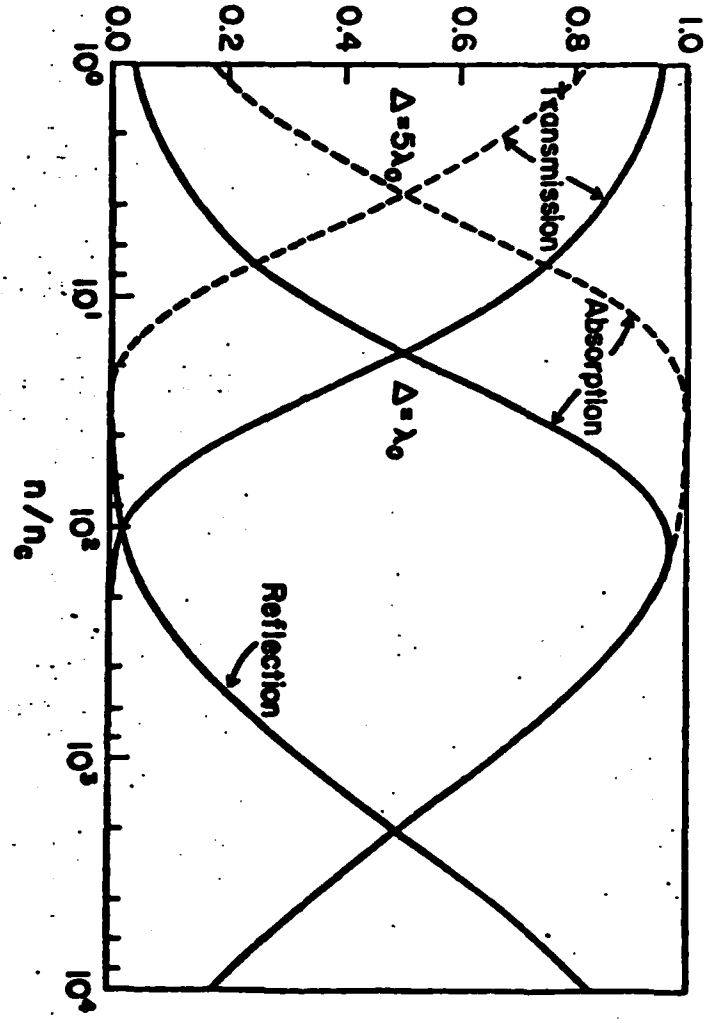

FIGURE 4

Absorption, transmission and reflection of microwaves as functions of maximum density for a plasma slab of width λ_o and 5 λ_o. This is a very collisional case that has the same p, f and I as in Figure 1.

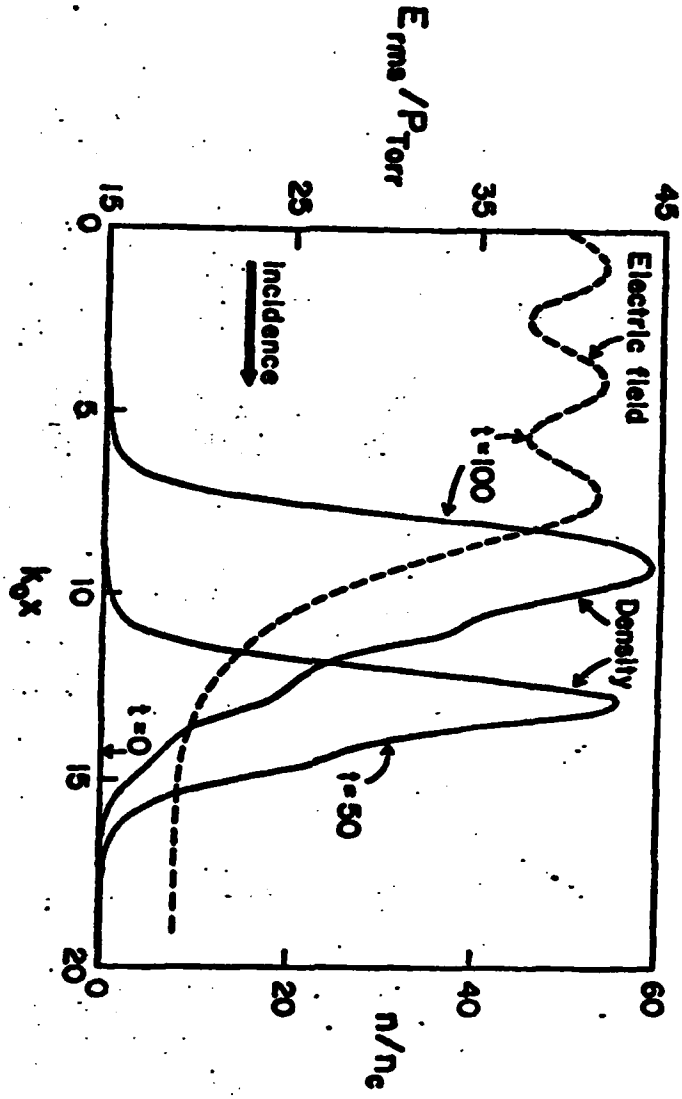

FIGURE 5

Density and microwave profiles at different times (in nsec). The initial pre-ionized localized density $n/n_c = 1$ is indicated by an arrow, and it evolves to an asymptotic density profile ($t = 100$) that moves rapidly toward the microwave source. This is a very collisional case that has the same p, f and I as in Figure 1.

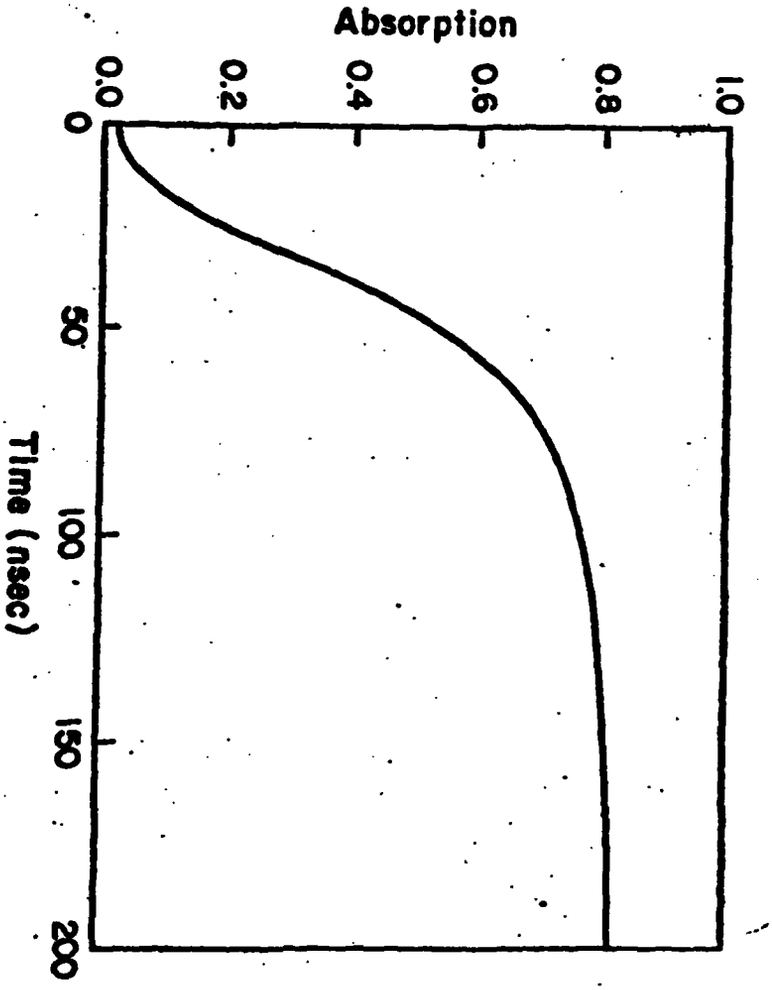

FIGURE 6

Time history for microwave absorption. Same case as in Figure 5.

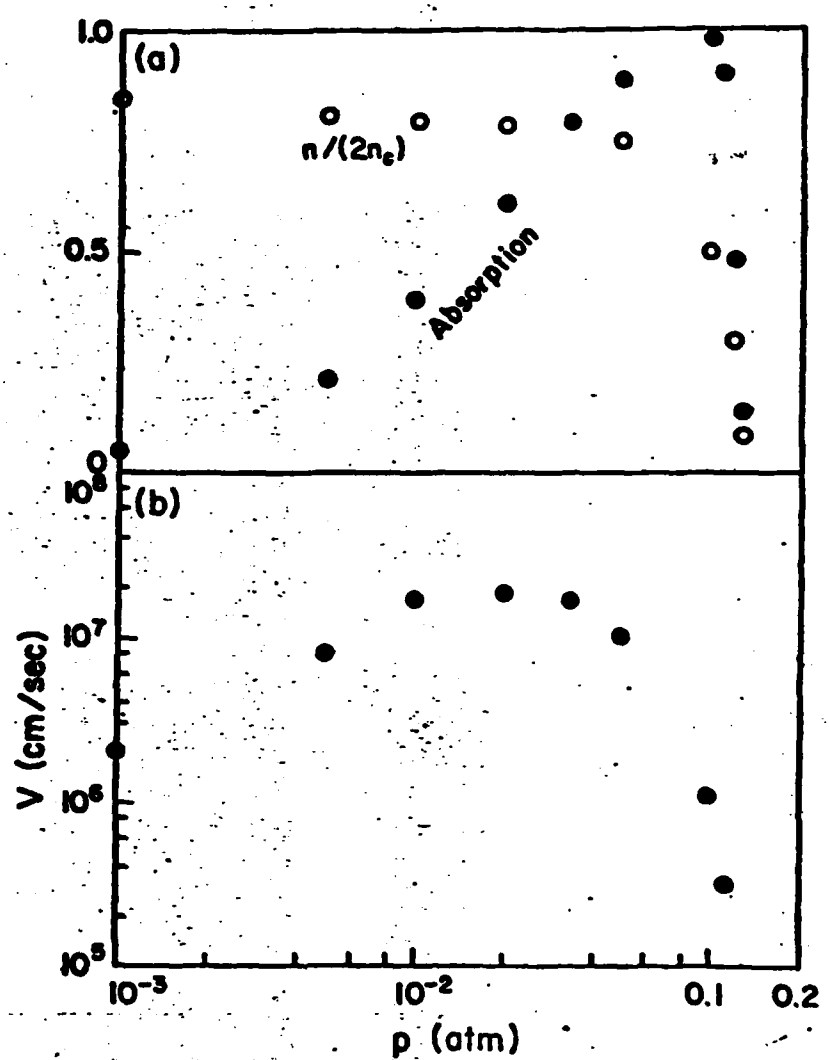

FIGURE 7

Asymptotic values obtained in runs with f = 35 GHz, I = 33 KW/cm^2, and initially pre-ionized density n = 0.1 n_c with width 0.25 λ_o. The system is weakly collisional for $P_{atm} \ll 0.1$. Displayed are: (a) Maxmimum density and absorption, and (b) speed of the ionization front as functions of pressure.

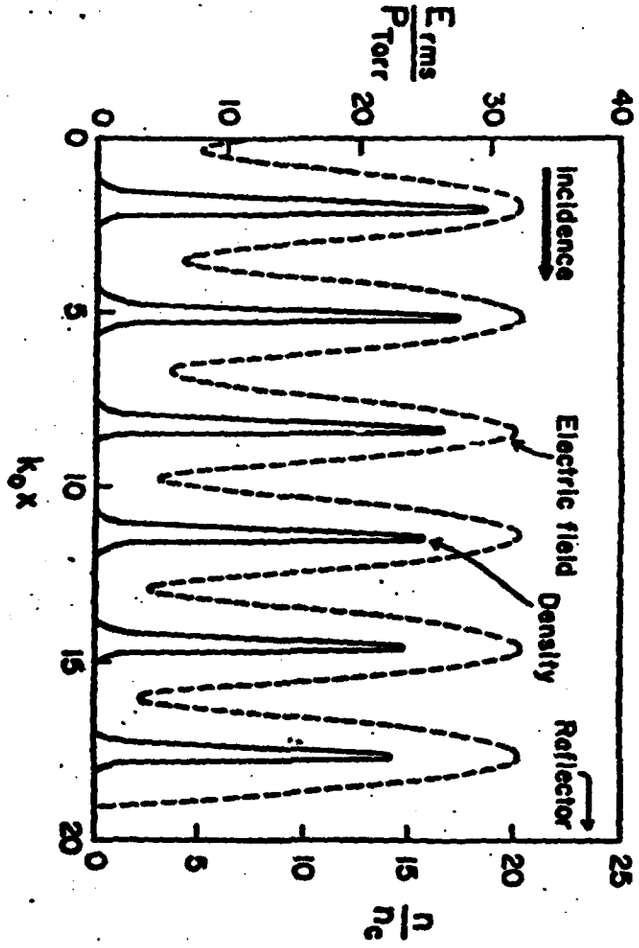

FIGURE 8

Density and microwave profiles at t = 200 nsec. A stationary state is achieved by using a reflector at the right such that only the initial maxima of the standing microwaves are above the breakdown threshold. This is a very collisional case with p = 1 atm, f = 3.2 GHz and I = 0.62 MW/cm^2.

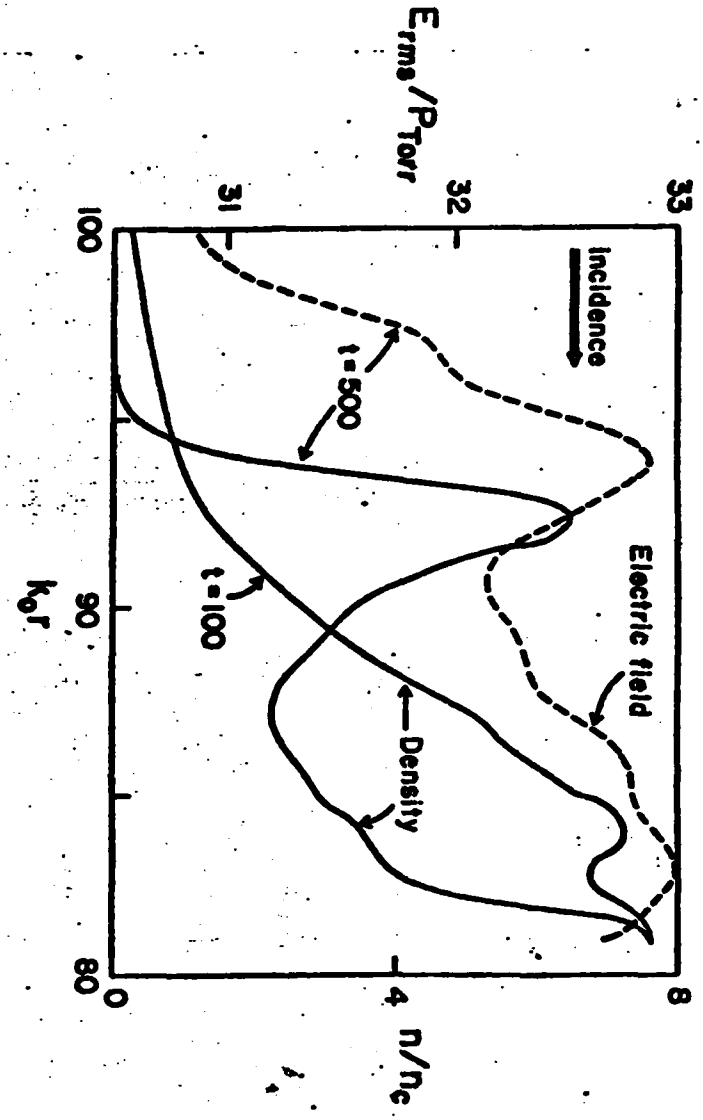

FIGURE 9

Density and microwave profiles at two different times (in nsec) for spherical geometry. Density peak is created at far right and moves to near the left edge where the microwave flux is below the breakdown threshold. This is a very collisional case with p = 1 atm, f = 3.2 GHz and I = 1.45 MW/cm^2.

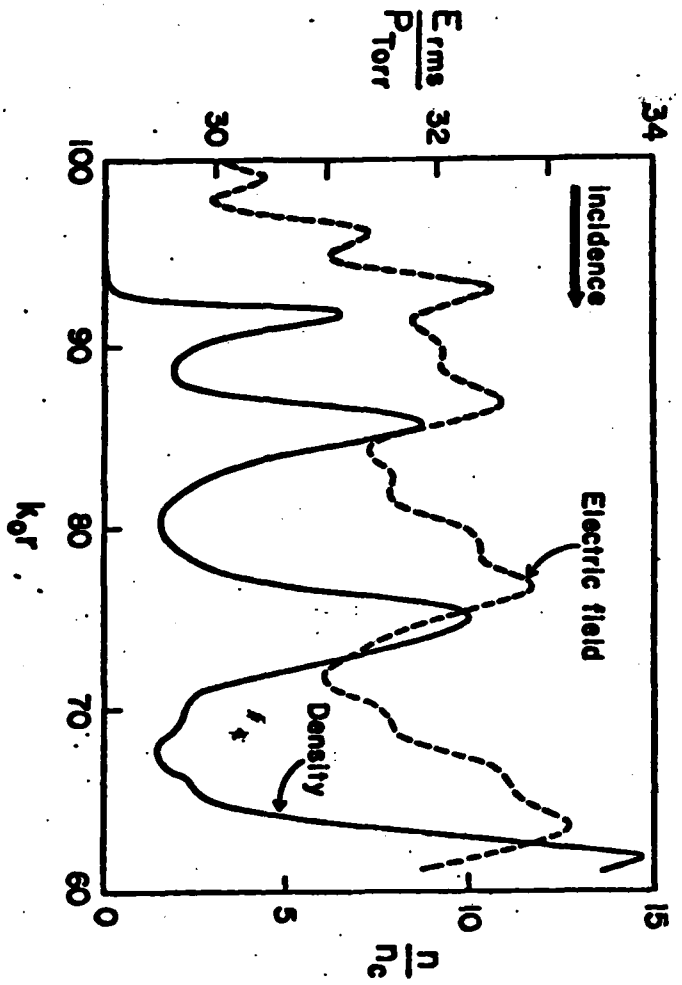

FIGURE 10

Density and microwave profiles at t = 1250 nsec for the system twice as long as that in Fig. 9. Many density peaks are created at far right and bunch up near the left edge. Note that the microwaves are attenuated to the breakdown value.

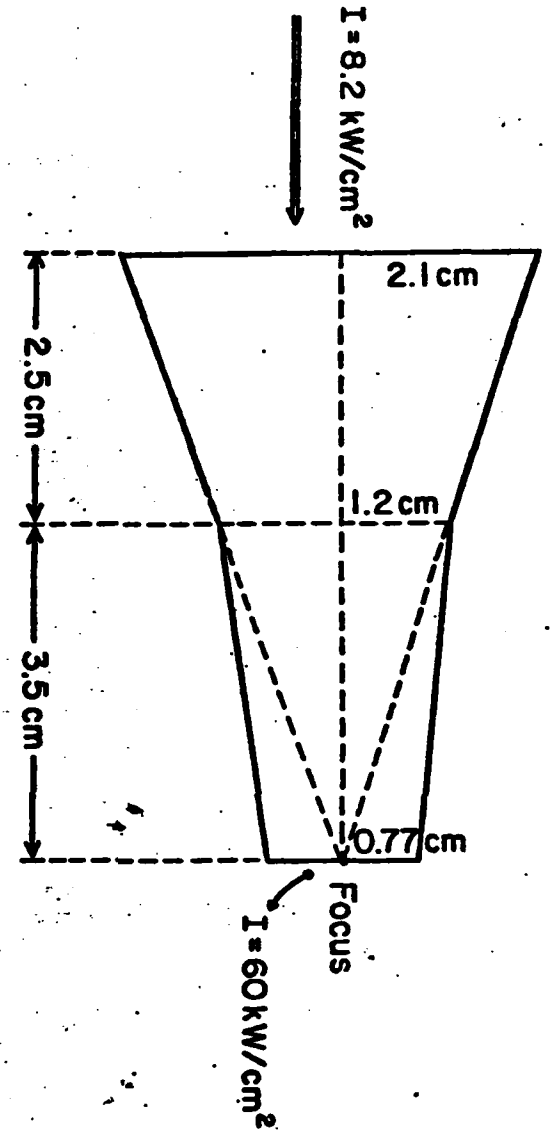

FIGURE 11

Schematic of the geometry for calculations to simulate the focused microwave experiments with p = 25 Torr, f = 35 GHz and power 112 kW. The estimated power fluxes on the axis are shown and diffraction (simulated by another spherical effect) starts roughly 3.5 cm from the focus.

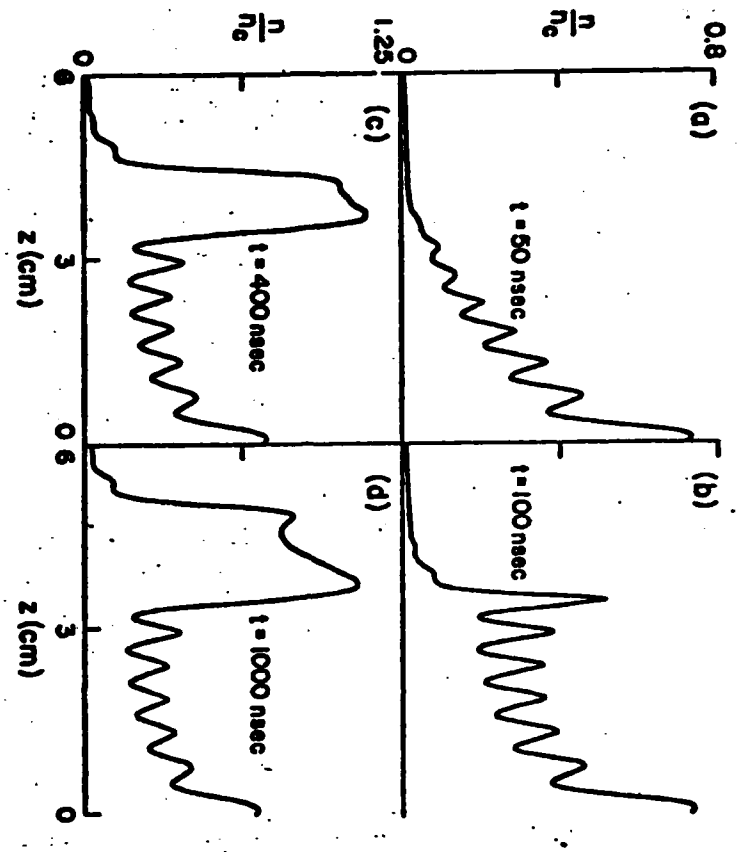

FIGURE 12

Density profiles at 4 different times for the case without reflector. The ionization occurs initially near the focus, however, the focal region is decoupled from the microwaves due to the stronger ionization near the connection region at later time.

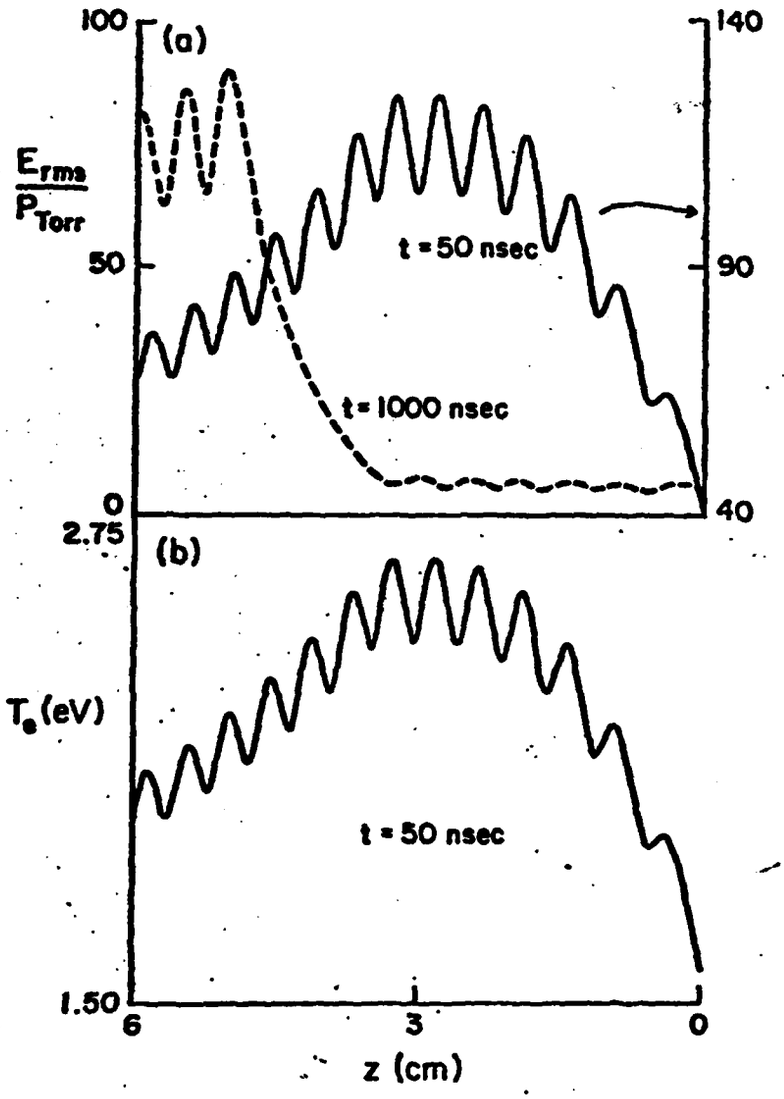

FIGURE 13

Microwave and temperature profiles corresponding to the plots shown in Figure 12. Microwaves are decoupled from the focal region as shown at t = 1000 nsec.

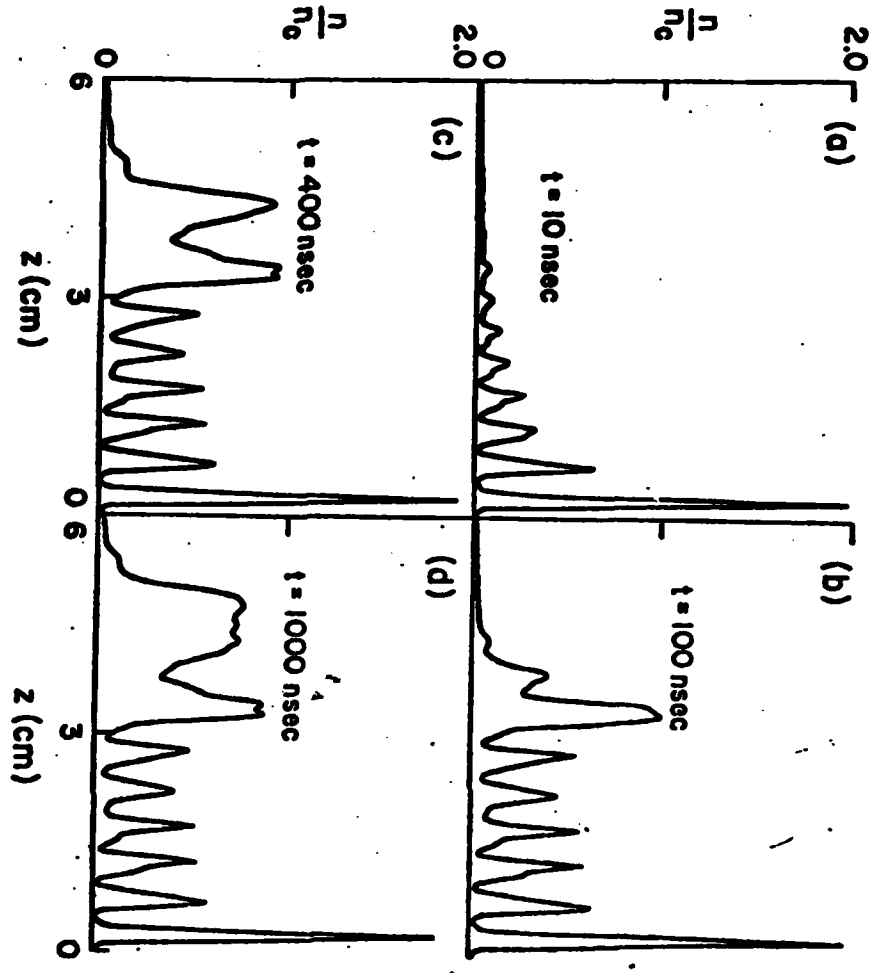

FIGURE 14

Density profiles at 4 different times for the case with a reflector at focus. A spiky structure is observed in this case.

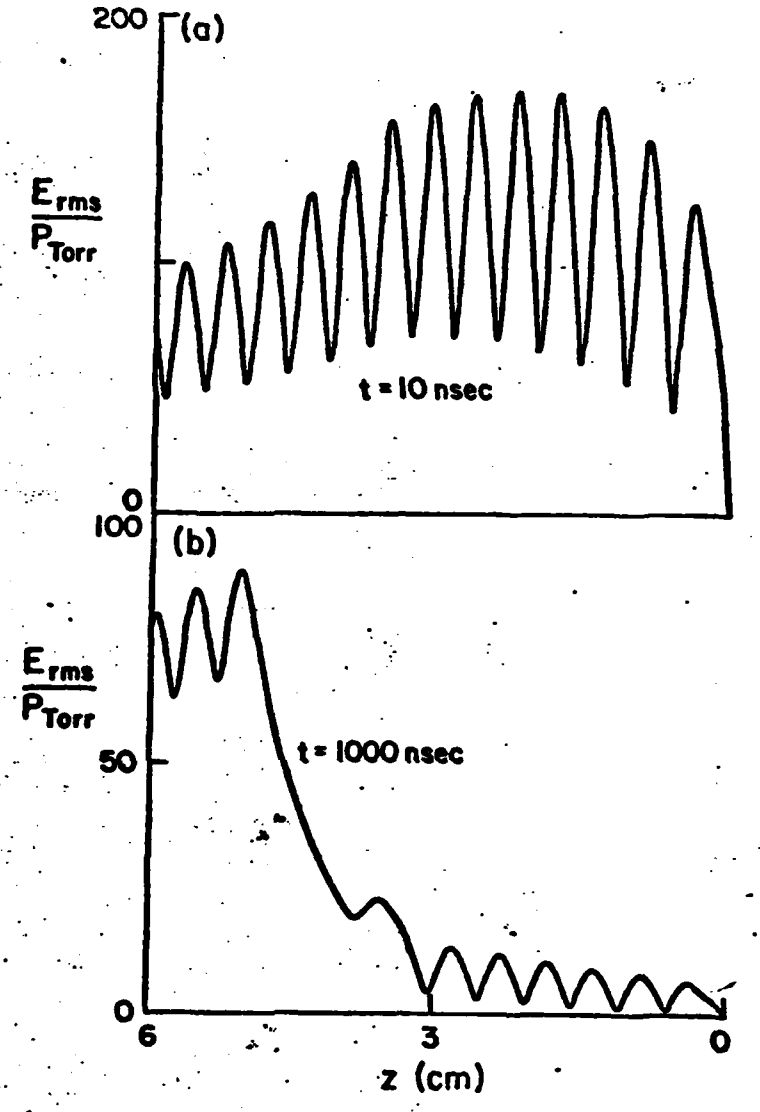

FIGURE 15

Microwave profiles corresponding to the plots in Figure 14.

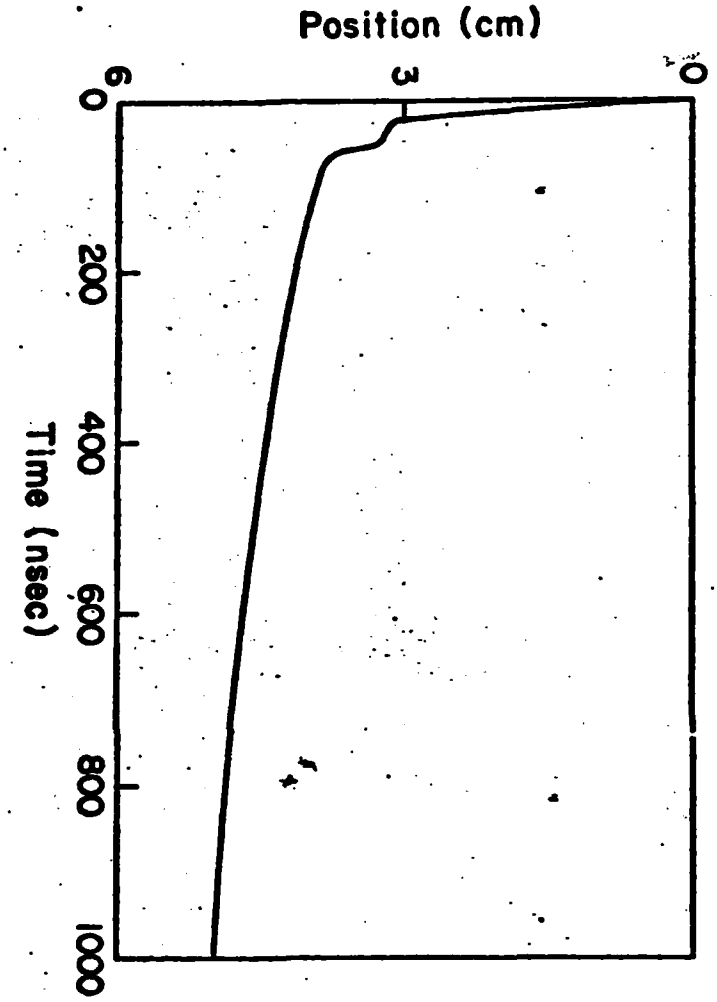

FIGURE 16

Time history of the position of the maximum of the microwave electric field. This shows the microwaves are decoupled quickly at about 50 nsec and the ionization front moves very slowly near the connection region.

END

FILMED

02 — 84

DTIC